

On the Number of Comets Around White Dwarf Stars: Orbit Survival During the Late Stages of Stellar Evolution

Joel Parriott

Department of Astronomy, University of Michigan
Ann Arbor, MI 48109
joelp@astro.lsa.umich.edu

and

Charles Alcock

Institute of Geophysics and Planetary Physics, Lawrence Livermore National Laboratory
Livermore, CA 94550
alcock@igpp.llnl.gov

ABSTRACT

The accretion of comets onto DA white dwarfs can produce observable metal absorption lines. We show here that comet systems around the progenitor main sequence star are vulnerable to being lost during asymptotic giant branch mass loss, if the mass loss is sufficiently asymmetric to impart modest linear momentum to the white dwarf. This may have bearing on the frequency of observation of heavy elements in white dwarf stars, and on inferences regarding the frequency of comet systems, if the imparted linear velocities of white dwarfs can be estimated.

Subject headings: comets: general — stars: white dwarfs — stars: mass loss — circumstellar matter — planetary systems

1. Introduction

The current model for solar system comets, based upon the classic theory of Oort (1950), contends that a vast cloud of cometary objects orbits the sun, and that this cloud consists of three components. The first, most inner, component is a disk-like structure of $\gtrsim 10^{10}$ comets referred to as the Kuiper belt (Edgeworth 1949; Kuiper 1951). The Kuiper belt has been proposed as the source for the Jupiter-family short-period (SP) comets, and to lie about $40 - 10^3$ AU from the sun (see Weissman 1995, and Luu *et al.* 1997). The second component, referred to as the inner Oort cloud (or “Hills” Cloud; Hills 1981), is believed to be a large fatter disk containing $10^{12} - 10^{13}$ objects lying $\sim 10^3 - 2 \times 10^4$ AU from the sun. The Hills Cloud is proposed as a source for both long-period (LP) and Halley-type SP comets (Levison 1996). The third component, is the classical

Oort cloud (Oort 1950). It is a roughly spherical cloud of $10^{11} - 10^{12}$ cometary objects, has a nearly isotropic velocity distribution, and extends from 2×10^4 to 2×10^5 AU. This component, which is physically contiguous with the Hills Cloud, yet dynamically distinct from it, is postulated to be a reservoir of LP comets which are brought into the inner solar system by perturbations due to passing stars, molecular clouds, and the galactic tidal field. It is likely that comets from the more populous Hills cloud region are continuously replenishing the randomized orbits of the outer Oort cloud, which are more easily lost from the stellar system due to their susceptibility to perturbation. While the formation history of the outer Oort cloud is disputed, the inner two components are thought to have formed out of the proto-planetary disk. For a further discussion of these topics and more, see these excellent reviews and references therein (Duncan and Quinn 1993; Weissman 1996; Levison 1996). This paper concerns the cloud components responsible for the LP comets, since they are the objects most likely to remain bound to the stellar system for the entire evolution of the central star.

It is reasonable to suppose that similar cometary systems exist around other stars given quite particular formation conditions (Tremaine 1993; Shull and Stern 1995); however, the cold, diffuse nature of such an Oort-type cloud would make it very difficult to directly detect (Stern, Shull, and Brandt 1990; Stern, Stocke, and Weissman 1991). Dust shells (eg. α Lyr) and disk-like structures (eg. β Pic), have been observed, via infrared excess, around $\lesssim 10\%$ of nearby stars (Aumann *et al.* 1984; Aumann 1985; Walker and Wolstencroft 1989; Aumann and Probst 1991; Oudmaijer *et al.* 1992; Zuckerman 1993; Lagrange-Henri 1995; Plets *et al.* 1997). These shells and disks may contain cometary material and planets, but definitive proof of the presence of extra-solar comets is elusive (Weissman 1984; Harper, Lowenstein, and Davidson 1984; Matese, Whitmore, and Reynolds 1989; Zuckerman and Becklin 1993; Beust *et al.* 1994; Hubeny and Heap 1996; Grady *et al.* 1997). The direct detection of Hills Cloud and Kuiper-type cometary systems around nearby stars is made more promising by the rapid evolution of technologies such as improved infrared detectors, new large infrared-optimized ground-based telescopes, adaptive optics, high-altitude and space-based infrared telescopes, and (sub-)millimeter arrays (Cruikshank, Werner, and Backman 1994; Burrows *et al.* 1995; Roddier 1995; Shao 1996; Holland *et al.* 1997). While the detection of these inner cometary systems, coinciding with large planets, may indirectly point to the presence of an Oort-type cloud, the null direct detections of a large outer cloud may continue. Given such an apparent impasse for direct observation, this work concerns possible implications for the indirect detection of Oort-type comet clouds around other single intermediate mass stars. These stars should end up as white dwarfs during the normal stellar evolutionary sequence.

Alcock, Fristrom, and Siegelman (1986, hereafter AFS) proposed that the accretion of a massive comet (e.g. $\sim 10^{17}$ g) onto a white dwarf star could raise the heavy element abundances above detection limits in the nearly pure hydrogen spectrum of a DA white dwarf. Most white dwarfs have hydrogen-rich atmospheres (DA) or helium-rich atmospheres (DB), which show no evidence for, or very low abundances of, elements heavier than hydrogen or helium. (For a good review of the optical characteristics and classification system of white dwarfs, see Wesemael *et al.*

(1993). The presence of metals, yet very little hydrogen, in DB stars is not well understood, and so we concern ourselves with the relatively simple DA/DAZ stars.) The dearth of detectable metals in DA and DAZ white dwarfs is believed to be caused by gravity-driven diffusive sedimentation of the heavier elements down out of the atmosphere (Alcock and Illarionov 1980a; Vauclair, Vauclair, and Greenstein 1979; Fontaine and Michaud 1979). According to the updated calculations of Paquette *et al.* (1986), the time scale for this metal diffusion process is on the order of 10^4 yr for a cool ($T_{\text{eff}} \sim 10,000$ K) DA white dwarf appropriate to the AFS analysis. Despite the rare appearance of metal lines in cool DA white dwarfs, several groups have made recent successful detections. The following papers contain metal abundances for DA/DAZ stars which are cool enough ($T_{\text{eff}} \lesssim 12,000$ K) to be of interest in this work, because their diffusion time scales are comparable to the comet accretion time scale: Dupuis, Fontaine, and Wesemael (1993); Shipman *et al.* (1995); Bergeron, Ruiz, and Leggett 1997; Koester, Provencal, and Shipman (1997); and Billères *et al.* (1997).

The signature of comets around white dwarfs depends on two properties of the intermediate temperature DA and DAZ stars. The first is the short sedimentation time, which implies that any heavy elements seen in the atmosphere are not primordial and must have been added recently. The second property of white dwarfs invoked by AFS is the small mass ($\lesssim 10^{23}$ g) of the atmosphere and outer convective envelope of these white dwarfs. Given their small atmospheres, the mass of material accreted need not be very large in order to produce detectable metal lines within the remarkably pure hydrogen spectrum. The accretion of one large comet can add enough material to be observed in this manner.

It should be pointed out that interstellar grain accretion is the standard explanation for the presence of calcium and magnesium lines in cool white dwarfs. The most recent work on the accretion-diffusion model for white dwarfs can be found in Dupuis *et al.* (1992, 1993). Major objections to this model have been raised by Aannestad *et al.* (1993), who cannot account for observed absolute calcium abundances given the low density interstellar medium around the solar neighborhood white dwarfs. They calculate limits on calcium accretion rates that are several orders of magnitude too low for observed abundances (cf. Alcock and Illarionov 1980b).

AFS point to the detection of calcium in the cool DAZ white dwarf G74 - 7 ($T_{\text{eff}} \sim 7000$ K; Lacombe *et al.* 1983) as an example of a possible recent accretion of a circumstellar comet, rather than the presumably negligible accretion of interstellar material (Alcock and Illarionov 1980b). (A very recent abundance determination for G74 - 7 can be found in Billères *et al.* (1997).) Using Joss's (1974) estimate of the rate of accretion of such a massive comet onto the Sun of 10^{-2}yr^{-1} , and the observed flat distribution of comet orbits in periastron distance (Fernandez 1982), AFS estimated that the rate of comet accretion onto a white dwarf (with radius $\sim 0.01R_{\odot}$) surrounded by an Oort-type cloud and planetary system similar to that of the solar system should be $\sim 10^{-4}\text{yr}^{-1}$. Since the estimated time between accretions is of the same order as the diffusion time for a cool DA star, one would expect that a white dwarf with an Oort-type cloud should maintain detectable metal lines for a significant fraction of its lifetime. Given the metal

abundances, one can place limits on the accretion rate from such a cloud and therefore define limits on the size of the cometary system surrounding the white dwarf.

AFS investigated the survival of a LP comet cloud population around a white dwarf during the periods of vigorous mass loss and very high luminosity through the post-asymptotic giant branch and pre-planetary nebula phases. Short-period comets at Kuiper belt distances from the star would be destroyed during this evolution (Stern, Shull, and Brandt 1990). AFS integrated orbits of LP comets (with a distribution similar to that inferred for the outer Oort cloud) in a stellar system which undergoes a gradual, spherically symmetric mass loss, with the mass of the central star given as a function of time, $M(t)$. They found that even when a significant fraction a star’s mass is lost during the pre-white dwarf phase of its evolution more than half of the comets in high-eccentricity, LP orbits remain bound, providing a supply of star-grazing comets which can be accreted by the star. The main physical reason for this result is that these comets spend most of their time at apastron, where they are more insensitive to changes in the potential energy of the system due to their low kinetic energy, and where they are out of danger of evaporation by the central star during its highly luminous red giant phase. The semi-major axes of the orbits increase due to the decreasing depth of the potential well of the system, but they do remain bound.

An important assumption made by AFS was that the mass loss during the advanced stages of stellar evolution is spherically symmetric. However, even a modest recoil velocity (~ 100 m/s) of the central star due to an asymmetry in the mass loss can be comparable to the speed of a comet near apastron, and as such should not be neglected when studying the survivability of such comets. Numerous observational studies of late-type stars and planetary nebulae have found that the majority of these objects show a dramatic departure from spherical symmetry (eg. Zuckerman and Aller 1986; Balick 1987; Bujarrabal, Alcolea, and Planesas 1992; Plez and Lambert 1994; Kastner *et al.* 1996; Manchado *et al.* 1996). For some recent HST results, see Sahai *et al.* (1997), Trammell and Goodrich (1997), and Sahai *et al.* (1998). While most planetary nebulae are aspherical, they typically have a high degree of other forms of intrinsic symmetry, such as elliptical, bipolar, and point-symmetry (see a review by Pottasch 1995, and references therein; Manchado, Stanghellini, and Guerrero 1996; Górny, Stasińska, and Tyłenda 1997). There are also a small number of objects which have no clear morphological symmetry, and are classified as “irregular.” The formation and evolution conditions that lead from relatively spherical red giants to the diverse morphologies of planetary nebulae is a matter of active research, and beyond the scope of this paper. We are interested in irregularities and departures from perfect symmetry, and the bipolar proto-planetary nebula OH 231.8+4.2 is an extreme case of such an imperfection. It has been shown that while OH 231.8+4.2 is axially symmetric, its two lobes differ *intrinsically* from one another (eg. Kastner *et al.* 1992; Alcolea, Bujarrabal, and Sánchez Contreras 1996). Alcolea, Bujarrabal, and Sánchez Contreras (1996) find that the southern lobe is 20% more massive than the northern lobe. Such a significant departure from symmetry is rare, but only small differences are required to impart the recoil velocities of interest in this paper. The model fits to apparently symmetric morphologies are not absolutely perfect, and it is conceivable that small intrinsic asymmetries, at levels well below

those seen in OH 231.8+4.2, have been going undetected in other objects.

In this work we extend the calculation of AFS to account for a simple asymmetric mass loss. Such a mechanism imparts a net impulsive linear momentum to the central star, which, as mentioned above, is important once its magnitude becomes comparable to the speed of a comet at apastron. We investigate the interesting parameter space of the problem, using Monte Carlo simulations, to identify when the mass loss rate, and thus the impulse velocity of the star, becomes large enough to significantly reduce the number of comets able to survive the mass loss.

In § 2 we present the calculation used to model the effects of asymmetric mass loss on an initial distribution of comet orbits similar to that of the Oort-cloud. The results of this calculation, in terms of the survivability of these comet orbits given a wide set of parameters that we feel covers the interesting parameter space of the problem, are presented in § 3. Finally, in § 4 we discuss the implications of these calculations for researchers in the field interested in the probability that a population of star-grazing comets could survive an asymmetric mass loss, given a knowledge of the conditions of the post asymptotic giant branch stage of a given star’s evolution.

2. Modeling the Asymmetric Mass Loss and Comet Ejection

We are interested in investigating the implications for an initial distribution of comet orbits, similar to those one would expect from an Oort-type cloud, when the central star of the system undergoes a smooth asymmetric mass loss. The asymmetric mass loss manifests itself by providing a net impulsive rectilinear acceleration to the central potential of the system. Of particular interest is the magnitude of this impulsive force necessary to unbind even the high-eccentricity long-period comet orbits, which proved to have a high survival rate for the spherically symmetric mass loss in AFS.

We treat the rectilinear acceleration due to the asymmetric mass loss as an additive fictitious force per unit mass \mathbf{f}_r in the equation of motion for the comet. The magnitude of this fictitious force is proportional to the mass loss rate, which one would qualitatively expect, and to the total velocity change of the star during the mass loss phase. For simplicity, the magnitude and direction of the mass loss are taken to be constant for the entire mass loss interval. Since the mass loss is not restricted to the initial orbital plane, angular momentum is not conserved, and the motion in the direction perpendicular to the plane must be included. The vector form of the equation of motion, realized in the instantaneous rest frame of the star, becomes

$$\frac{d^2\mathbf{r}}{dt^2} = -\frac{GM(t)\mathbf{r}}{r^3} - \mathbf{f}_r, \quad \text{where } \mathbf{f}_r = \Delta\mathbf{v} \frac{\dot{M}(t)}{M_f - M_i}. \quad (1)$$

$\Delta\mathbf{v}$ represents the total velocity change imparted to the star, due to this rectilinear acceleration, during the mass loss phase. For $M(t)$ we assume the smooth analytic mass loss function used by

AFS, which has the form

$$M(t) = \frac{1}{2}(M_i + M_f) - \frac{1}{2}(M_i - M_f) \tanh \frac{2t}{T}, \quad (2)$$

where M_i is the initial mass, M_f is the final mass, and T is the mass loss interval. We concern ourselves with the time interval $-3T < t < 3T$, so that the time of vigorous mass loss is included fully and the error in the initial and final masses falls below one part in 10^4 . $\dot{M}(t)$ is then obtained by differentiation of equation (2).

We choose to parameterize the total impulsive velocity of the star $\Delta \mathbf{v}$ in terms of the ratio of the semi-major axis of the orbit a to the period P multiplied by a dimensionless factor Λ :

$$\Delta \mathbf{v} = \Lambda \frac{a}{P} \hat{\mathbf{n}}, \quad (3)$$

where $\hat{\mathbf{n}}$ is a unit vector in the direction of the rectilinear acceleration (opposite the direction of the mass loss). This is a convenient scale because a/P is of the same order as the characteristic velocity of the problem, i.e. the average velocity of a comet around its orbit. An impulsive velocity imparted to the star which is much larger than this characteristic velocity would be expected simply to separate the star from the slowly moving cometary system, and a much smaller velocity would have negligible influence on the state of stellar system. The interesting effects for this occur when $\Lambda \sim 1$.

The dynamical equations (1) are invariant under the transformation:

$$\begin{aligned} M &\longrightarrow \gamma M \\ \mathbf{r} &\longrightarrow \xi \mathbf{r} \\ t &\longrightarrow \xi^{\frac{3}{2}} \gamma^{-\frac{1}{2}} t \\ \Delta \mathbf{v} &\longrightarrow \xi^{-\frac{1}{2}} \gamma^{\frac{1}{2}} \Delta \mathbf{v} \\ \dot{M}(t) &\longrightarrow \xi^{-\frac{3}{2}} \gamma^{\frac{3}{2}} \dot{M}(t). \end{aligned} \quad (4)$$

Units for the computation were selected such that the initial $a = GM = 1$ for each orbit integration, and so the initial period of the orbit $P = 2\pi$. The initial conditions of each comet orbit are then completely determined by the eccentricity squared e^2 , and the starting phase w_3 (the fractional area of the ellipse since the last periastron; Goldstein 1981).

If one starts with a particular choice of a physical problem $(a_i, \Delta \mathbf{v}, M_f, M_i, \dot{M}_{\max})$, the transformation to the units used in the code, as given by this formalism, is

$$\gamma = (GM_i)^{-1}, \quad (5)$$

$$\xi = a_i^{-1}; \quad (6)$$

therefore,

$$\Lambda = \Delta \mathbf{v} \frac{\dot{M}_{\max}}{M_i - M_f} \frac{a_i^2}{GM_i}, \quad (7)$$

where \dot{M}_{\max} is the maximum value of the mass loss rate (functionally, the value of $\dot{M}(t)$ at $t = 0$). For example, one obtains $\Lambda \approx 6.7$ for the following set of typical parameters: $a_i = 10^4 AU$, $\Delta v = 300 \text{m/s}$, $M_i = 2M_\odot$, $M_f = 0.8M_\odot$, $\dot{M}_{\max} = 10^{-4}M_\odot/\text{yr}$. The calculation of the fraction of comet orbits which remain bound after the mass loss, B , versus the ratio of the initial period to the mass loss interval, P/T , corresponding to these parameters can be found by interpolating between the second and third column plots of Figure 4, given an orbit eccentricity. We address these plots fully in Section III.

In order best to simulate the physical nature of the problem, Monte Carlo techniques were used to provide a random initial w_3 and mass loss direction for each integration. Since a random direction for the mass loss is used, the inclination of the initial orbital plane is removed from the problem. To \sqrt{N} accuracy, the distribution of initial comet orbits is uniform with respect to w_3 and the mass loss direction on the sphere, where $N = 10,000$ for all of the calculations shown in this paper.

The equation of motion of an orbit was integrated as a function of time in Cartesian coordinates, using an adaptive time step, fourth order Runge-Kutta method. The code was tested by integrating Kepler orbits, with the mass of the star remaining fixed, and further by reproducing the results of AFS in the spherical mass loss case ($\Lambda = 0$).

3. Results

We begin by obtaining the value of the energy of a comet at the end of each orbit integration, E_f , as a function of the initial phase, w_3 , for each parameter set: e^2 , $\Delta \mathbf{v}$, P/T , and M_f/M_i . The fraction of orbital initial phase with $E_f > 0$ represents the fraction of comets which have become unbound and escaped from the system. For each set of integrations we determine the fraction of comets that remain bound after mass loss, which we will denote by B . The values of E_f versus w_3 lie on a single smooth curve for the symmetric mass loss case ($\Delta \mathbf{v} = 0$; see AFS); however, the final energy curves become much more complex once the asymmetric mass loss is introduced.

Figure 1 contains representative plots of this E_f versus w_3 relationship for a specific set of parameters. The calculation in Figure 1(a) corresponds to the case where the direction of the mass loss (opposite the direction of the rectilinear acceleration) is restricted to the direction of initial apastron in the initial orbital plane. Roughly 2/3 of the orbits in this case have become unbound ($E_f > 0$), and the bound orbits are found toward the middle range of w_3 . The curve is quite smooth in the region $0.35 < w_3 < 0.85$, but spikes appear outside this range. In Figure 1(b), we incorporate the entire randomness of both direction and initial phase for the same set of parameters as in Figure 1(a). Note the filling of the $E_f - w_3$ parameter space bounded by seemingly smooth curves. Closer observation also reveals two bounding curves at work on the top edge of the region for $w_3 < 0.5$. The extrema of E_f as well as the location of the global minimum are the same as in Figure 1(a). There are also a greater fraction of bound orbits in this case than

for the restricted direction case. The full Monte Carlo realization of the calculation introduces an entirely new level of complexity and richness to the problem.

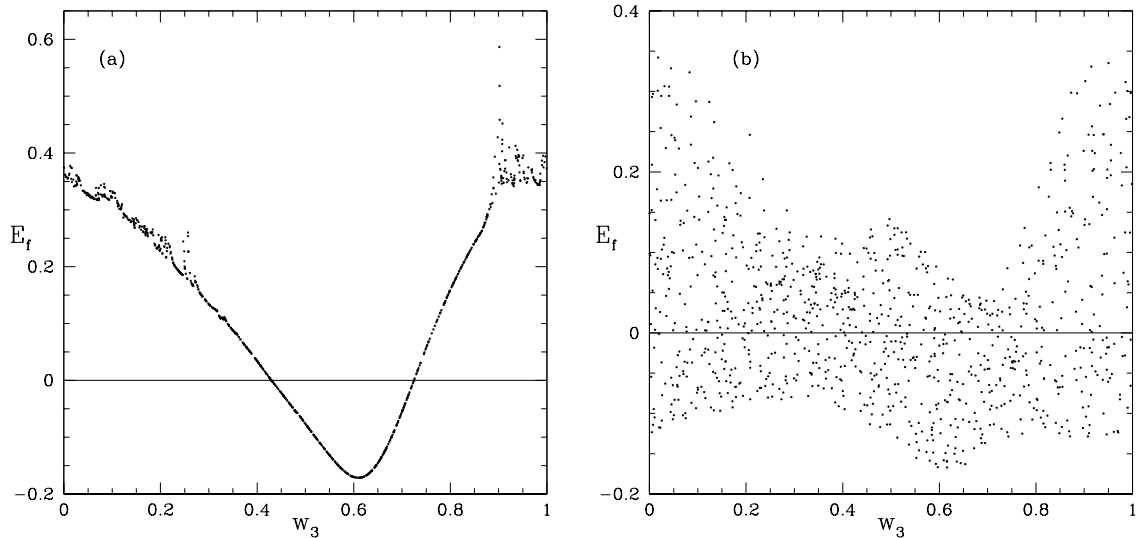


Fig. 1.— The final energy of an orbit as determined by the initial phase w_3 (the fraction of the area of the orbital ellipse from periastron at the start of the integration). Since $GM = a = 1$, the initial energy of all comets is $E = -0.5$. (a) Mass loss restricted to the direction of initial apastron for all w_3 . Squared eccentricity $e^2 = 0.8$, multiplicative factor of the mass loss $\Lambda = 4$, mass ratio $M_f/M_i = 0.4$, and period to mass loss interval ratio $P/T = 0.9$. (b) Fully random simulation (both w_3 and direction) for the same parameters as in (a). Note change in abscissa scale.

We repeat these calculations for different values of P/T in order to sample different periods in terms of the mass loss interval. In Figures 2-6 we show mosaics of plots of the bound fraction of comets B as a function of the initial period to mass loss interval ratio P/T , for different mass loss ratios. The bound fraction obtained from each plot similar to that in Figure 1(b) then represents a single point in these figures. The values lie on a smooth curve, and the \sqrt{N} fluctuations are approximately the same size as the dots on the plot. As was the case for symmetric mass loss, small values of P/T approximate the adiabatic limit, where the mass loss takes place very slowly. Large values of P/T represent the sudden mass loss approximation (Hills 1983), and the points asymptotically approach the line representing this limit, as expected. In order to verify that the limit is truly achieved in every case, we carried out full calculations increasing P/T up to a value of 2000 and found each asymptote to be correct. In the energetically susceptible orbit region around $P/T \approx 1$ we see a minimum in the curve, as in the case for symmetric mass loss, but the additional structure present in that region is quite interesting, yet unexplained physically. Even considering the random fluctuations introduced by the Monte Carlo techniques, the structure

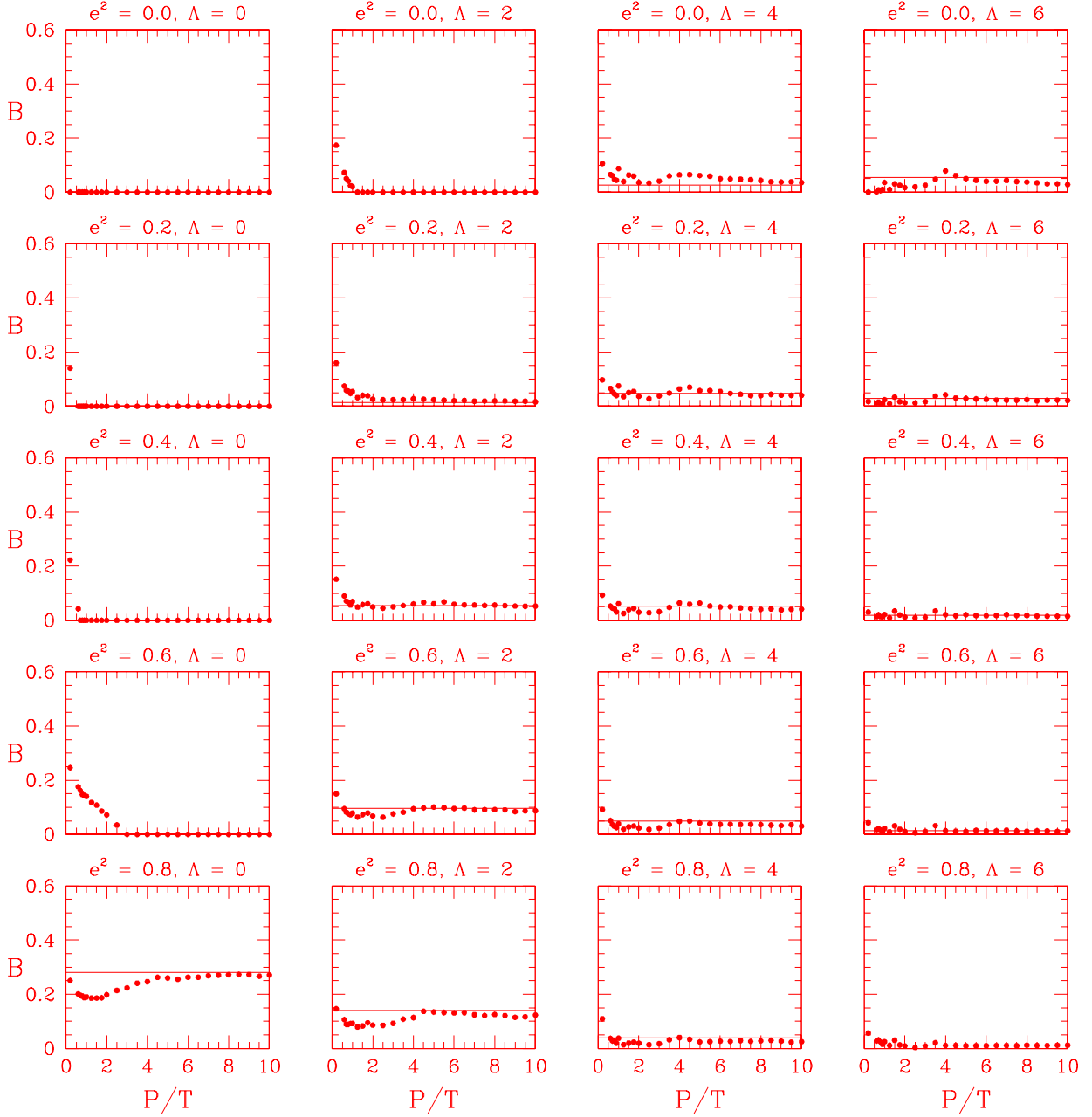


Fig. 2.— The probability B that a comet remains bound as a function of the ratio of initial period P to mass loss interval T . This mosaic represents a large parameter space range of initial squared eccentricities e^2 and multiplicative factors for the mass loss Λ , for a mass ratio $M_f/M_i = 0.1$. The \sqrt{N} random errors are represented by the size of the points, and the same error exists for the line.

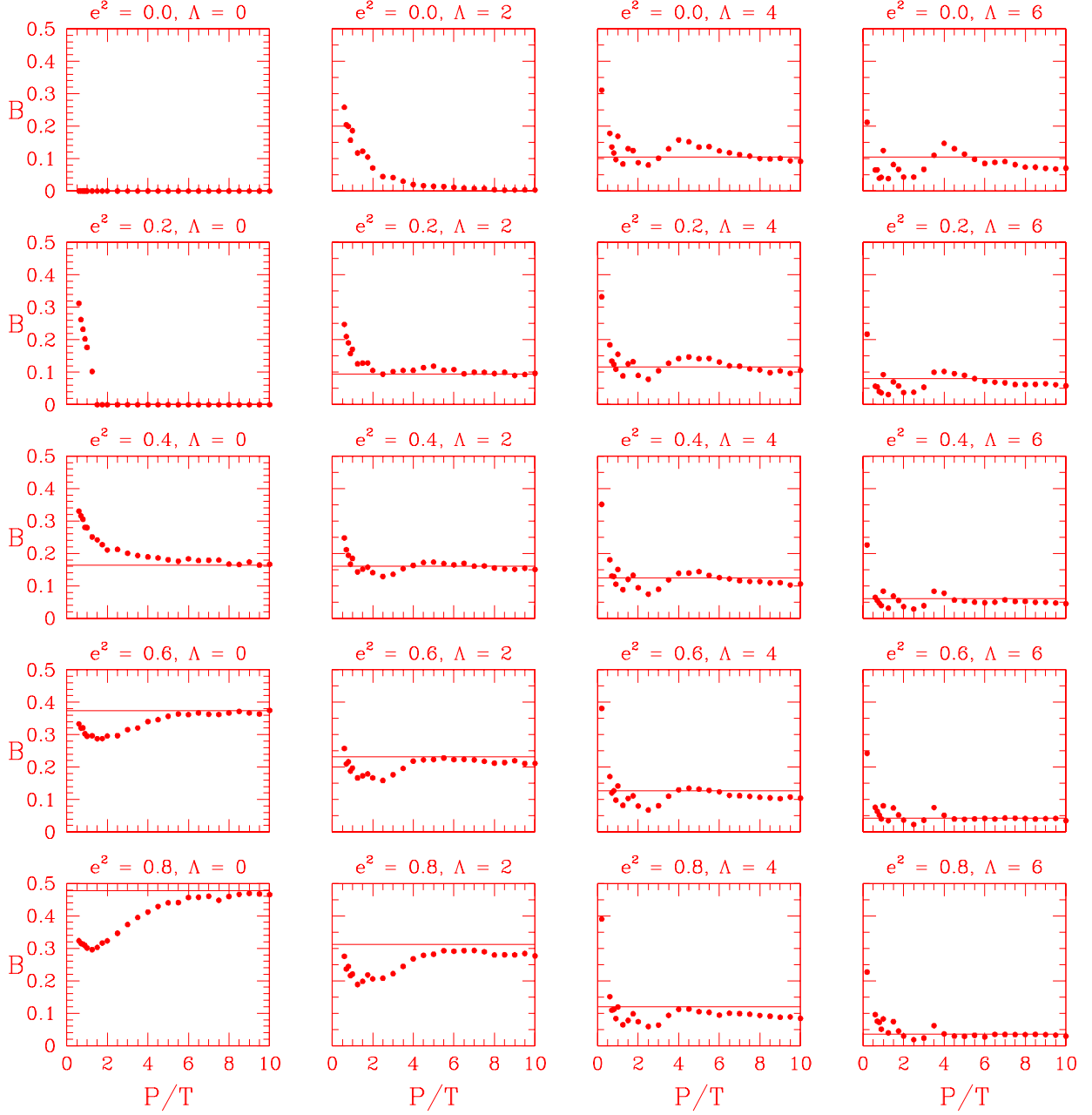


Fig. 3.— A mosaic similar to that in figure 2, for a mass ratio $M_f/M_i = 0.2$. Note change in abscissa scale.

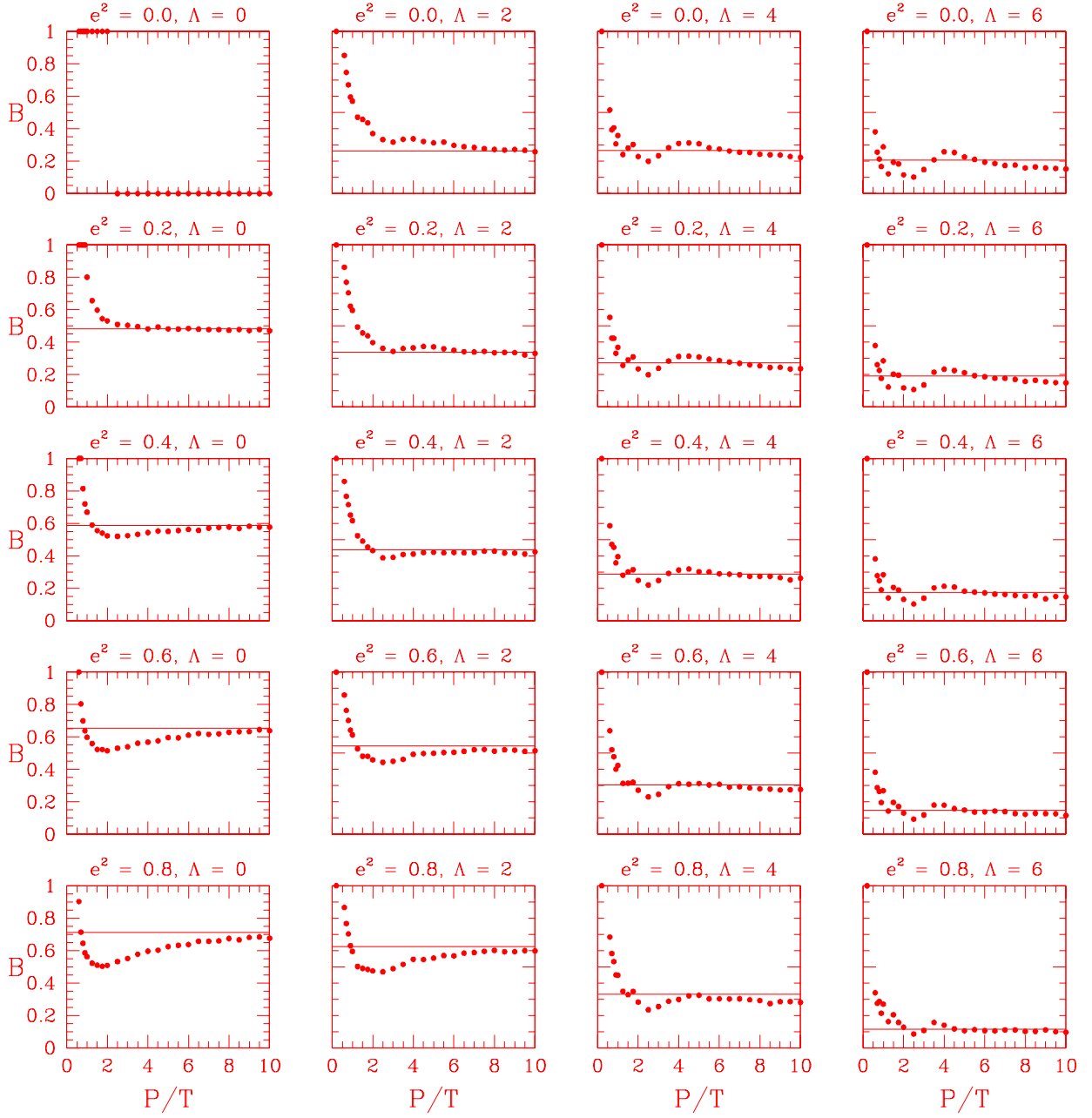


Fig. 4.— A mosaic similar to that in figure 2, for a mass ratio $M_f/M_i = 0.4$. Note change in abscissa scale.

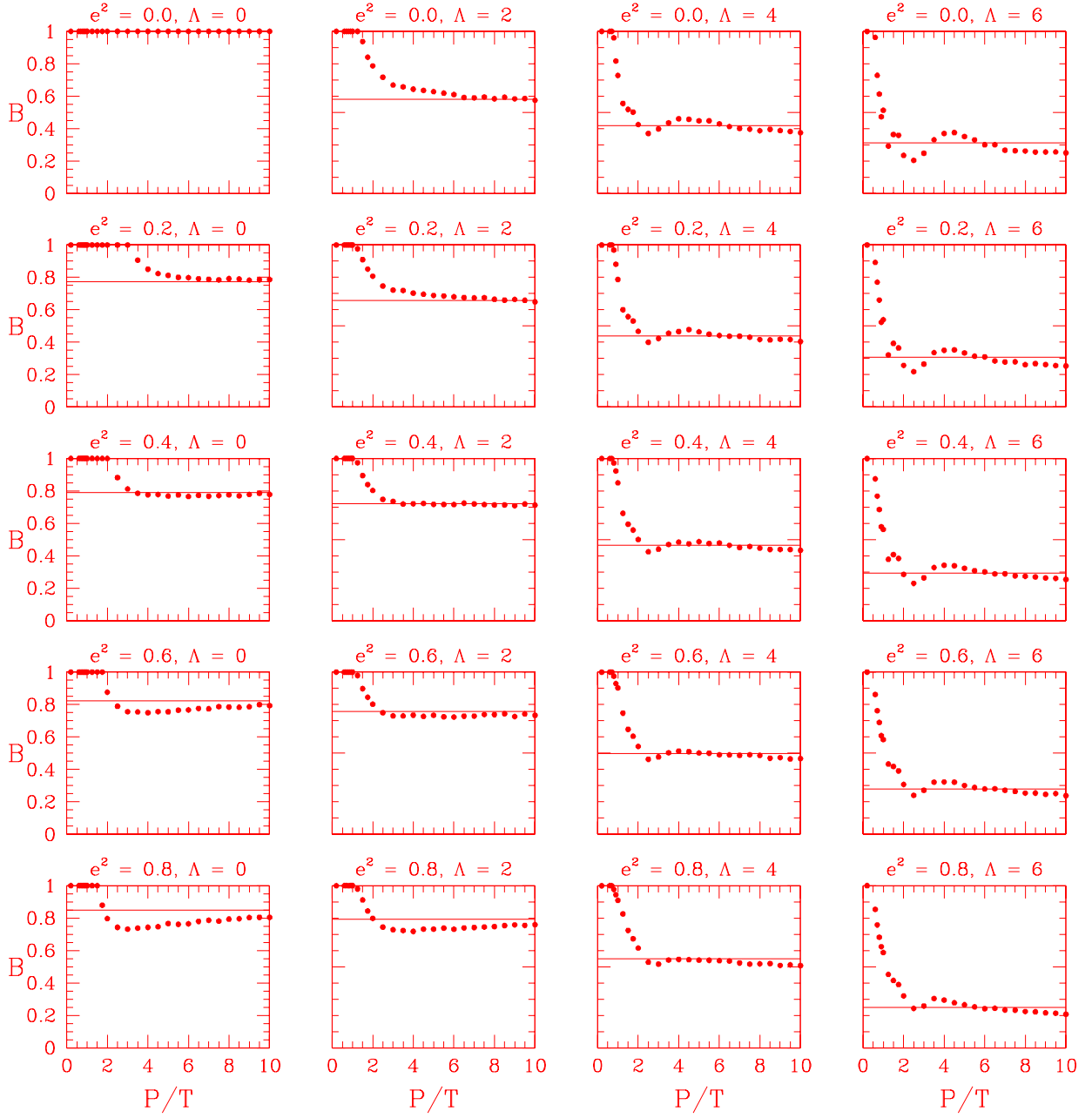


Fig. 5.— A mosaic similar to that in figure 2, for a mass ratio $M_f/M_i = 0.6$. Note change in abscissa scale.

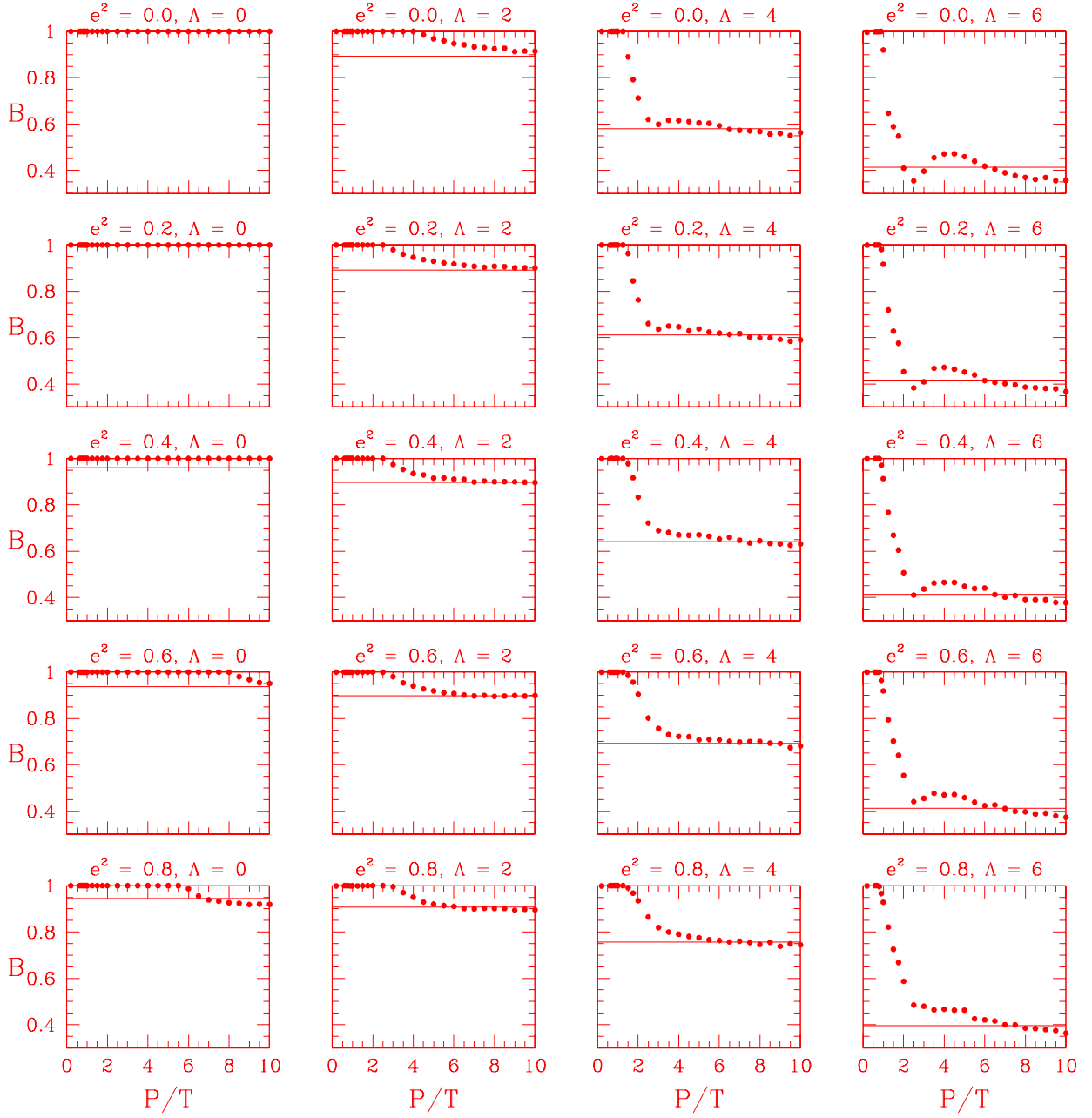


Fig. 6.— A mosaic similar to that in figure 2, for a mass ratio $M_f/M_i = 0.8$. Note change in abscissa scale.

is real. We believe that these mosaics provide a coverage of the interesting parameter space relevant to this calculation, in terms of the strength of the mass loss, mass loss ratios, and initial eccentricities. With such a representation of different scenarios, one can see the cases where a significant number of comets will remain in order to become probable future star-grazers for the white dwarf. As was the case for symmetric mass loss, it is precisely the highly eccentric orbits which remain more bound as the magnitude of the rectilinear acceleration increases. The strength of the mass loss, given the scaling of the mass loss amplitude used, need not become very large in order to lose most of the comets.

The behavior of the asymptotic sudden mass loss limits also possesses some interesting details. In Figures 7 & 8 we have plotted these asymptotes as a function of the multiplicative factor, Λ , for the range of eccentricities, e^2 , shown in the mosaics, but only for $M_f/M_i = 0.2$ & 0.6 respectively. These two mass loss fractions represent two interesting cases in terms of the observations of the masses white dwarfs in clusters where a main sequence turn-off point can be found, thereby allowing an estimate of the mass of the white dwarf progenitor to be found. The case of $M_f/M_i = 0.2$ is believed to be about the maximum mass loss observed; the case in point is the white dwarf Sirius-B, which has a mass of $1.1M_\odot$ and is in a cluster with a turn off mass of $6.0M_\odot$. A $M_f/M_i = 0.6$ is about the mass loss fraction expected for $1.0M_\odot$ stars. Both cases show very smooth curves which for the most part have the bound asymptote decreasing monotonically with increasing Λ . Both also show apparent convergent point(s), near $\Lambda = 4 - 5$, which have a spread in B that is not significant within \sqrt{N} errors.

An interesting feature of Figure 7 is the maximum in asymptote at this convergent point for circular and nearly circular orbits, yet one would intuitively expect the sudden mass loss limiting value for the surviving comets monotonically to decrease as the effects of asymmetric mass loss become stronger (i.e. increasing impulse velocity of the central star). This can be explained because a certain fraction of the comet orbits have initial velocities in the same direction as the rectilinear acceleration, and as such they can “catch up” to the star for small to medium values of this acceleration. Once the the acceleration becomes large enough they can no longer catch up.

Also note that the ordering from most bound fraction to least, for the given eccentricities, flips order at the convergent point(s). At lower Λ , the higher the eccentricity the larger the bound fraction, but at higher Λ , the lower the eccentricity, the larger the bound fraction. The circular orbits in Figure 8 do not follow this general trend at small Λ ; they have a larger bound asymptotic value than some or all of the more elliptical orbits, and the effect must be interpreted as genuine because it is not within random errors. $M_f/M_i = 0.6$ is the intersection of much of the characteristic phase space for this problem, and so effects such as this are not easily isolated.

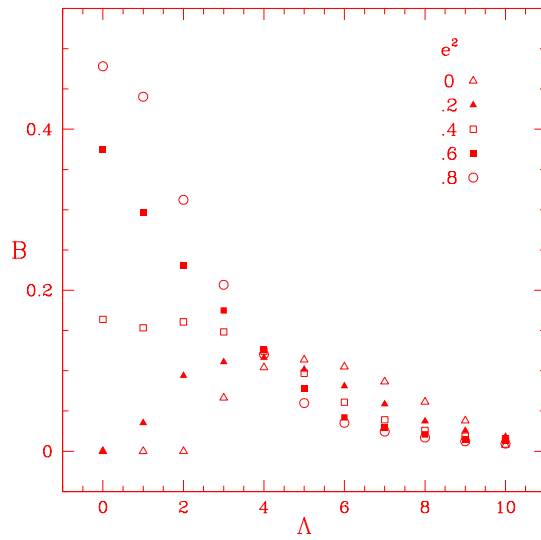


Fig. 7.— The value of B for the sudden mass loss approximation asymptote as a function of the mass loss multiplicative factor Λ , for the values of e^2 represented in the mosaics, and for $M_f/M_i = 0.2$.

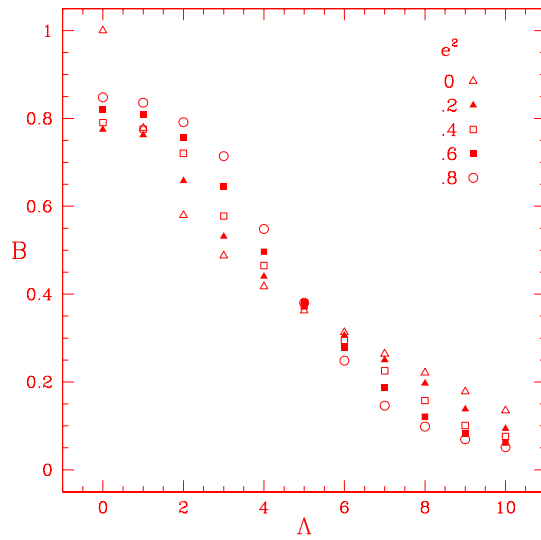


Fig. 8.— Similar to figure 7, for $M_f/M_i = 0.6$. Note change in abscissa scale.

4. Discussion and Conclusions

The results of these simulations will be useful to the reader interested in knowing the likelihood that a population of star-grazing long-period comets could have survived the mass loss stages of the white dwarf under study. We have covered a large parameter space and provided a direct scaling relationship between our calculations and appropriate physical properties of a given physical system. Comet survival can be estimated given the comet’s initial orbital eccentricity and semi-major axis and a knowledge of the star’s post asymptotic giant branch evolution: progenitor initial mass, maximum mass loss rate, net recoil velocity (if any) due to asymmetric mass loss, and final white dwarf mass. We calculated an example given some typical numbers for the above quantities and found a scaling that was well within the simulation parameter space.

We have performed calculations in order to determine the effects of a simple model for stellar asymmetric mass loss on an initial distribution of comet orbits for a system similar to the solar system. Asymmetric mass loss may explain the very small fraction ($< 10\%$) of white dwarfs with detectable metals when potential cometary systems are detected around a larger fraction ($\sim 10\%$) of nearby main sequence stars, given the accretion signature theory of AFS. Our calculations show that an impulsive velocity of the central star of only a few hundred m/s is enough to even drastically reduce the number of long-period, star-grazing comets in an Oort-type cloud population.

CA wishes to thank Jim Liebert for a useful discussion. We would also like to thank Ben Zuckerman for his helpful comments. JP was supported in part by the Computational Science Graduate Fellowship Program of the Office of Scientific Computing in the Department of Energy. Research at LLNL is supported under Contract W-7405-ENG from the Department of Energy.

REFERENCES

- Aannestad, P. A., Kenyon, S. J., Hammond, G. L., & Sion, E. M. 1993, *AJ*, 105, 1033
- Alcock, C., Fristrom, C. C., & Siegelman, R. 1986, *ApJ*, 302, 462 (AFS)
- Alcock, C., & Illarionov, A. 1980a, *ApJ*, 235, 534
- . 1980b, *ApJ*, 235, 541
- Alcolea, J., Bujarrabal, V., & Sánchez Contreras, C. 1996, *A&A*, 312, 560
- Aumann, H. H. 1985, *PASP*, 97, 885
- Aumann, H. H. & Probst, R. G. 1991, *ApJ*, 368, 264
- Aumann, H. H., et al. 1984, *ApJ*, 278, L23
- Balick, B. 1987, *AJ*, 94, 671
- Bergeron, P., Ruiz, M. T., & Leggett, S. K. 1997, *ApJS*, 108, 339
- Beust, H., Vidal-Madjar, A., Ferlet, R., & Lagrange-Henri, A. M. 1994, *Ap&SS*, 212, 147
- Billères, M., Wesemael, F., Bergeron, P., & Beauchamp, A. 1997, *ApJ*, 488, 368
- Bujarrabal, V., Alcolea, J., & Planesas, P. 1992, *A&A*, 257, 701
- Burrows, A., Saumon, D., Guillot, T., Hubbard, W. B., & Lunine, J. I. 1995, *Nature*, 375, 299
- Cruikshank, D. P., Werner, M. W., & Backman, D. E. 1994, *Ap&SS*, 212, 407
- Duncan, M., & Quinn, T. 1993, *ARA&A*, 31, 265
- Dupuis, J., Fontaine, G., & Wesemael, F. 1993, *ApJS*, 87, 345
- Dupuis, J., Pelletier, C., Fontaine, G., & Wesemael, F. 1992, *ApJS*, 82, 505
- . 1993, *ApJS*, 84, 73
- Edgeworth, K. E. 1949, *MNRAS*, 109, 600
- Fernandez, J. A. 1982, *AJ*, 87, 1318
- Fontaine, G., & Michaud, G. 1979, *ApJ*, 231, 826
- Goldstein, H. 1980, *Classical Mechanics* (2nd ed.; Reading: Addison-Wesley), 472
- Górny, S. K., Stasińska, G., & Tylenda, R. 1997, *A&A*, 318, 256
- Grady, C. A., Sitko, M. L., Bjorkman, K. S., Pérez, M. R., Lynch, D. K., Russell, R. W., & Hanner, M. S. 1997, *ApJ*, 483, 449
- Harper, D. A., Lowenstein, R. F., & Davidson, J. A. 1984, *ApJ*, 285, 808
- Hills, J. G. 1981, *AJ*, 86, 1730
- . 1983, *ApJ*, 267, 322
- Holland, W., et al. 1997, *BAAS*, 191, #47.06
- Hubeny, I., & Heap, S. R. 1996, *ApJ*, 470, 1144

- Joss, P. C. 1974, *ApJ*, 191, 771
- Kastner, J. H., Weintraub, D. A., Gatley, I., Merrill, K. M., & Probst, R. G. 1996, *ApJ*, 462, 777
- Kastner, J. H., Weintraub, D. A., Zuckerman, B., Becklin, E. E., McLean, I., & Gatley, I. 1992, *ApJ*, 398, 552
- Koester, D., Provencal, J., & Shipman, H. L. 1997, *A&A*, 230, L57
- Kuiper, G. P. 1951, in *Astrophysics*, ed. J. A. Hynek (New York: McGraw-Hill), 357
- Lacombe, P., Liebert, J., Wesemael, F., & Fontaine, G. 1983, *ApJ*, 272, 660
- Lagrange-Henri, A.-M. 1995, *Ap&SS*, 223, 19
- Levison, H. F. 1996, in *ASP Conf. Proc. 107, Completing the Inventory of the Solar System*, ed. T. W. Rettig, & J. M. Hahn (San Francisco: ASP), p. 173
- Luu, J., Marsden, B. G., Jewitt, D., Trujillo, C. A., Hergenrother, C. W., Chen, J., & Offutt, W. B. 1997, *Nature*, 387, 573
- Manchado, A., Stanghellini, L., & Guerrero, M. A. 1996, *ApJ*, 466, L95
- Manchado, A., Guerrero, M. A., Stanghellini, L., & Serra-Ricart, M. 1996, *BAAS*, 189, #120.14
- Matese, J. J., Whitmore, D. P., & Reynolds, R. T. 1989, *Icarus*, 81, 24
- Oort, J. H. 1950, *Bull. Astr. Inst. Netherlands*, 11, 91
- Oudmaijer, R., van der Veen, W. E. C. J., Waters, L. B. F. M., Trams, N. R., Waelkens, C., & Engelsman, E. 1992, *A&AS*, 96, 625
- Paquette, C., Pelletier, C., Fontaine, G., & Michaud, G. 1986, *ApJS*, 61, 197
- Plets, H., Waelkens, C., Oudmaijer, R. D., & Waters, L. B. F. M. 1997, *A&A*, 323, 513
- Plez, B., & Lambert, D. L. 1994, *ApJ*, 425, L101
- Pottasch, S. R. 1995, in *Asymmetrical Planetary Nebulae*, ed. A. Harpax & N. Soker, *Ann. Israel Phys. Soc.*, 11, 7
- Roddier, F. 1995, *Ap&SS*, 223, 109
- Sahai, R., et al. 1997, *BAAS*, 191, #15.08
- Sahai, R., Hines, D. C., Kastner, J. H., Weintraub, D. A., Trauger, J. T., Rieke, M. J., Thompson, R. I., & Schneider, G. 1998, *ApJ*, 492, L163
- Shao, M. 1996, *Ap&SS*, 241, 105
- Shipman, H. L., et al. 1995, *AJ*, 109, 1220
- Shull, J., & Stern, S. 1995, *AJ*, 109, 690
- Stern, S., Shull, J., & Brandt, J. 1990, *Nature*, 345, 305
- Stern, S., Stocke, J., & Weissman, P. 1991, *Icarus*, 91, 65
- Trammell, S. R., & Goodrich, R. W. 1997, *BAAS*, 191, #47.15

- Tremaine, S. 1993, in ASP Conf. Proc. 36, Planets Around Pulsars, ed. J. A. Phillips, J. E. Thorsett, & S. R. Kulkarni (San Francisco: ASP), p. 335
- Vauclair, G., Vauclair, S., & Greenstein, J. L. 1979, A&A, 80, 79
- Walker, H. J., & Wolstencroft, R. D. 1989, PASP, 100, 1509
- Weintraub, D., & Stern, S. 1994, AJ, 108, 701
- Weissman, P. 1984, Science, 224, 987
- . 1995, ARA&A, 33, 327
- . 1996, in ASP Conf. Proc. 107, Completing the Inventory of the Solar System, ed. T. W. Rettig, & J. M. Hahn (San Francisco: ASP), p. 265
- Wesemael, F., Greenstein, J. L., Liebert, J., Lamontague, R., Fontaine, G., Bergeron, P., & Glaspey, J. W. 1993, PASP, 105, 761
- Zuckerman, B. 1993, in ASP Conf. Proc. 36, Planets Around Pulsars, ed. J. A. Phillips, J. E. Thorsett, & S. R. Kulkarni (San Francisco: ASP), p. 303
- Zuckerman, B., & Aller, L. H. 1986, ApJ, 301, 772
- Zuckerman, B., & Becklin, E. E. 1993, ApJ, 414, 793